

Chemisorption-induced 4*f*-core-electron binding-energy shifts for surface atoms of W(111), W(100), and Ta(111)

J. F. van der Veen

FOM Institute for Atomic and Molecular Physics, Kruislaan 407, 1098 SJ Amsterdam, The Netherlands

F. J. Himpsel and D. E. Eastman

IBM Thomas J. Watson Research Center, Yorktown Heights, New York 10598

(Received 27 January 1982)

Hydrogen- and oxygen-induced chemical shifts have been resolved in Ta and W substrate 4*f* core levels by high-resolution synchrotron-radiation-excited photoemission spectroscopy. The surface levels shift continuously by typically 100 to 200 meV to higher binding energy for increasing hydrogen coverage. This is due to a quenching of surface states in the valence band and a charge transfer from the substrate to the hydrogen atoms. Upon adsorption of oxygen, new core peaks appear at 0.4 to 1.3 eV higher binding energy with respect to the bulk level, indicating the formation of strong chemisorption bonds. Substrate chemical shifts for element *Z* correlate with chemisorption-induced changes in the heat of surface segregation of the (*Z*+1) constituent in a dilute (*Z*+1)_{*x*}*Z*_{1-*x*} alloy.

I. INTRODUCTION

The use of x-ray photoelectron spectroscopy (XPS) for the study of chemical bonding at surfaces has gained widespread interest during the last decade.¹ Most of these investigations were concerned with the interpretation of chemical shifts in core levels from *adsorbate* atoms. By contrast, the effect of adsorption on *substrate* core levels has received much less attention. Yet, a measurement of chemical shifts in substrate atom core-level binding energies could provide valuable information on the nature of the chemical bond between adsorbate and substrate atoms, e.g., the number of surface atoms bonding to an adsorbate atom, and the amount of charge transfer involved. This may ultimately lead to a model for the binding site of the chemisorbed atom. Using surface-sensitive core-level spectroscopy, one can monitor different stages of oxygen chemisorption up to surface oxidation, and can study the mechanism of hydrogen uptake for a material like tantalum which is known to dissolve large amounts of hydrogen in the bulk. In most of the XPS work, using Al*Kα* or Mg*Kα* radiation, the main difficulty in resolving chemisorption shifts in substrate core levels has been a lack of sufficient energy resolution and depth resolution, although in some cases small shifts have been seen.^{2,3} However, for heavily oxidized W (Ref. 4) and Mo (Ref. 5) surfaces binding-energy shifts as large as several eV have been measured. With soft

x rays chemically shifted substrate core levels have also been observed during oxidation of Al,⁶ Si,⁷ and GaAs,⁸ for hydrogen saturated surfaces of W(111),⁹ Ta(111),⁹ and W(100),¹⁰ and recently for a *p*(2×1) ordered overlayer of oxygen on W(110).¹¹

In the present work we report chemical shifts in 4*f* core-level binding energies of surface atoms from W(111), W(100), and Ta(111), induced by hydrogen and oxygen chemisorption. These shifts have been resolved by the use of high resolution (150 meV) photoelectron spectroscopy at soft x-ray energies (*hν*~70 eV). At these photon energies the escape depth of W and Ta 4*f* electrons is very small [≤ 3 Å (Ref. 9)] resulting in high surface sensitivity. The 4*f*_{7/2} levels from Ta and W are well suited for monitoring chemical shifts, since they have a very small lifetime width (150 and 110 meV, respectively).

Recent experiments have shown that even for clean surfaces the top layer atoms have different core-level binding energies from bulk¹²⁻¹⁴ atoms. These intrinsic surface shifts arise from the fact that a surface atom has less neighbors than a bulk atom and are sensitively dependent on surface crystallography.¹⁴ Upon adsorption of hydrogen, the surface core levels for W(111) and Ta(111) shift toward larger binding energy by 150 and 250 meV, respectively, indicating an initial-state charge transfer in the valence band from the substrate atoms toward the hydrogen atoms. Most surprisingly, these levels shift continuously for increasing

hydrogen coverage, without significant loss of intensity. This behavior cannot be explained by a simple chemical bonding model—often used in XPS analysis of solids—in which the core-level binding energy directly reflects the *local* chemical environment. Rather, the continuous change in binding energy appears to correlate with hydrogen-induced quenching and lowering in binding energy of surface states in the valence band.

The bonding of oxygen is markedly different in its effect on surface atom core levels. A rapid quenching (and continuous shift) of the intrinsic surface levels is observed, while new chemically shifted substrate core peaks appear, which reflect different bonding configurations for the chemisorbed oxygen atoms.

The paper is organized as follows: Experimental measurement and surface preparation techniques are described in Sec. II. Section III presents substrate core-level shifts for W(111), W(100), and Ta(111) induced by hydrogen and oxygen adsorption. In Sec. IV we discuss the origin of substrate chemical shifts and their correspondence with heats of surface segregation. Also, the possible role of final-state relaxation effects is discussed.

II. EXPERIMENTAL

Angle-integrated photoemission spectra (collecting a cone of $\sim 87^\circ$ full angle around the sample normal) were taken with a display-type spectrometer¹⁵ and a toroidal grating monochromator at the Synchrotron Radiation Center of the University of Wisconsin. Photon energies (66–70 eV) were chosen such that escaping photoelectrons from Ta and W have a kinetic energy of ~ 35 –40 eV. Since the electron escape depth is small at these energies ($\lesssim 3 \text{ \AA}$), the core-level spectra contain an appreciable contribution from the outermost surface layers. The combined system resolution (monochromator plus spectrometer) was about 150 meV, as determined from the observed width of the Fermi level edge.

The W surfaces were cleaned by repeated oxidation at $\sim 1100 \text{ K}$, followed by flashing *in vacuo* to $> 2300 \text{ K}$. The Ta(111) crystal ($4.5 \times 2.5 \times 0.5 \text{ mm}^3$) was first outgassed in vacuum at $\sim 2300 \text{ K}$ for about an hour. After this treatment the main surface contaminant was found to be oxygen, which diffuses out of the bulk. After repeated flashes to 2500–2700 K the oxygen could be removed, resulting in a clean surface as judged by Auger spectroscopy and the absence of chemical-

shifted 4f surface core levels. The Ta(111), W(111), and W(100) surfaces all showed a sharp (1×1) low-energy electron diffraction (LEED) pattern, but for clean W(100) very weak and diffuse half-order spots were seen, indicative of a partly reconstructed surface.^{16,17} The working pressure in the chamber was in the low 10^{-11} -Torr range. Hydrogen and oxygen exposures are given in uncorrected ion-gauge readings.

III. CHEMICAL SHIFTS OF W AND Ta SUBSTRATE CORE LEVELS

A. W(111)+H₂

Angle-integrated photoemission curves for the W 4f_{7/2} core levels are shown in Fig. 1 for different hydrogen exposures, after subtraction of a linear secondary electron background (as in Ref. 9). Count rates in the 4f_{7/2} peak were typically

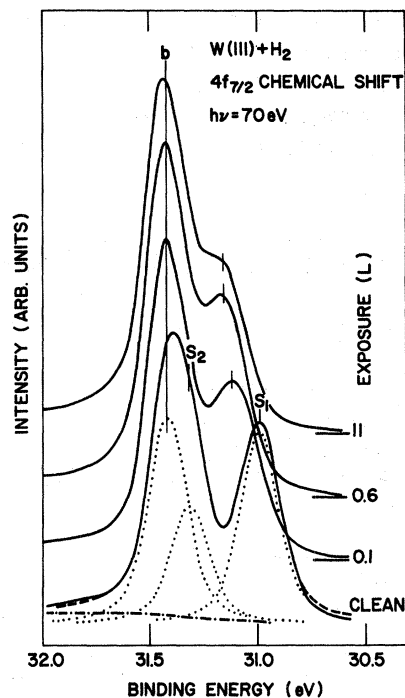


FIG. 1. Angle-integrated 4f_{7/2} core-level emission spectra for W(111) as a function of hydrogen exposure (solid lines). A linear background has been subtracted. Dotted curves show a best-fit decomposition into Lorentzian bulk (*b*) and surface core levels (*S*₁, *S*₂), convoluted with the instrumental resolution; a small background due to extrinsic losses is also shown (dash-dotted line). The result of our line-shape fit is shown by a dashed line only where it deviates from the experimental curve.

$5 \times 10^4 \text{ sec}^{-1}$, giving a signal-to-noise ratio of better than 200:1. Binding energies are referred to the Fermi level (E_F). The $4f_{5/2}$ levels at 2.16 eV higher binding energy are not shown since they are an exact replica of the $4f_{7/2}$ photoemission curves, apart from an additional lifetime broadening by $\sim 53 \text{ meV}$ (Table I) due to $\text{N}_6\text{N}_7\text{O}_{45}$ super-Koster-Kronig Auger decay processes. Previous photoemission measurements have demonstrated the existence of two surface core peaks (S_1 and S_2 in Fig. 1) for the clean W(111) surface, which are shifted to lower binding energies relative to the bulk level (b). These surface binding-energy shifts largely reflect initial-state changes in the electrostatic potential at the core due to charge transfer and are sensitively dependent on the surface atom coordination number.¹⁴ Core peak S_1 originates from the topmost surface layer and is shifted by 0.43 eV, while S_2 originates from atoms in the second (third) layer and differs in binding energy only by 0.10 eV with respect to the bulk core peak. As pointed out in Ref. 9, the existence of *two* surface core levels is related to the open structure of a W(111) surface (bcc lattice) for which atoms in the first, second, and third layer have four, seven, and seven nearest neighbors, compared with eight nearest neighbors for a bulk atom (Fig. 2).

Photoemission curves for clean and hydrogen-covered W(111) have been decomposed into bulk and surface contributions by a least-squares fitting procedure, in which each core level is represented by a Lorentzian, with full width at half maximum (FWHM) of 2γ and intensity as free parameters of the fit, convoluted with a Gaussian instrument function having a FWHM of 150 meV (in Fig. 1 only shown for the clean surface). Because of its reliability and its suppression of noise, we preferred this iterative convolution procedure above the alternative scheme of deconvoluting the experimental resolution function from the data prior to the fit. A small extrinsic background was also included in the fit (dash-dotted line in Fig. 1). Best-fit values for surface-to-bulk core-level binding-energy differences and lifetime widths are given in Table I.

Surface core levels S_1 and S_2 both shift to higher binding energy for increasing exposures of hydrogen (Fig. 1), while the bulk level (b) remains unaffected. Their sensitivity to chemisorption is direct evidence that S_1 and S_2 are originating from surface atoms. In particular the existence of S_2 is demonstrated. After 0.1-L exposure ($1 \text{ L} = 1 \times 10^{-6} \text{ Torr sec}$) S_2 becomes degenerate with the bulk level, giving rise to an apparent sharpening of this core peak and a small shift in its posi-

TABLE I. Summary of $4f$ core-level parameters for atoms of the first surface layer (S_1), second layer (S_2), and bulk (b) of Ta(111), W(111), and W(100). Binding energies are referred to the Fermi level. All energy values are in units of eV.

	Ta(111)	W(111)	W(100)
$4f_{7/2}$ bulk binding energies E_b	21.64±0.05	31.42±0.05	31.42±0.05
$4f_{5/2}4f_{7/2}$ spin-orbit splitting	1.90±0.01	2.16±0.01	2.16±0.01
Intrinsic $4f_{7/2}$ surface binding energy: E_{S_1}	22.04±0.05	30.99±0.05	31.07±0.05
E_{S_2}	21.83±0.05	31.32±0.05	
Intrinsic $4f$ surface binding-energy shift:			
$\Delta E_{S_1} = E_{S_1} - E_b$	0.40±0.01	-0.43±0.01	-0.35±0.01
$\Delta E_{S_2} = E_{S_2} - E_b$	0.19±0.02	-0.10±0.02	
$4f_{7/2}$ spectral width 2γ (FWHM): Bulk	0.15±0.02 ^a	0.11±0.02	0.11±0.02
Clean surface (S_1, S_2)	0.19±0.03 ^a	0.11±0.02	0.11±0.02
Extra lifetime broadening $4f_{5/2}$:			
$2\gamma(4f_{5/2}) - 2\gamma(4f_{7/2})$	0.036±0.010	0.053±0.015	0.053±0.015
Chemical shift for saturation coverage of hydrogen: $E_{S_1}(\text{H}) - E_{S_1}(\text{clean})$	0.25±0.02	0.17±0.02	0.095±0.02
$E_{S_2}(\text{H}) - E_{S_2}(\text{clean})$	0.17±0.02	~ 0.10	
Oxygen-induced binding-energy shifts in Figs. 6, 7, and 10: $E_A - E_b$	1.12±0.05	0.41±0.10	
$E_C - E_b$	1.3±0.1		0.53±0.05
$E_D - E_b$	2.4±0.1		
$E_E - E_b$	0.5±0.1		

^aTa $4f$ levels have a Doniach-Sunjić line shape with asymmetry parameter $\alpha = 0.06 \pm 0.03$ (Ref. 9).

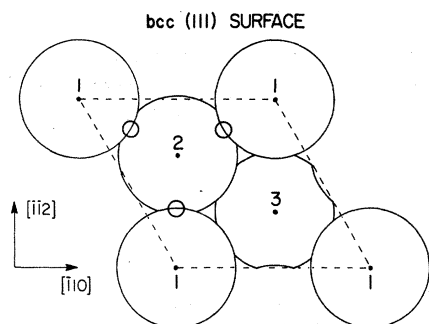


FIG. 2. Hard-sphere model of a (111) surface of a bcc crystal showing that three atomic layers are exposed. The most probable binding sites for bridge-bonded hydrogen atoms are also indicated (small circles).

tion. For this and higher exposures good fits have been obtained by using two-level decompositions into (bulk + S_2) and S_1 .

Figures 3 and 4 show best-fit values for the S_1 surface-to-bulk core-level binding-energy difference ΔE_{S_1} and surface-to-bulk peak area ratios $A_{S_1}/(A_b + A_{S_2})$ as a function of hydrogen exposure (solid circles). Figure 3 includes measurements for exposures below 0.1 L that are omitted from Fig. 1. The most notable feature is a *continuous* chemical shift of S_1 for increasing hydrogen coverage (here we define a chemical shift as the binding-energy difference between clean and adsorbate covered surface). The total chemical shift for S_1 after saturation with hydrogen (11-L exposure) amounts to 170 meV. Most of this shift (~ 120 meV) has already occurred after 0.1-L exposure, without any loss of intensity but with a minor broadening by 20–30 meV. An exposure of 0.1 L

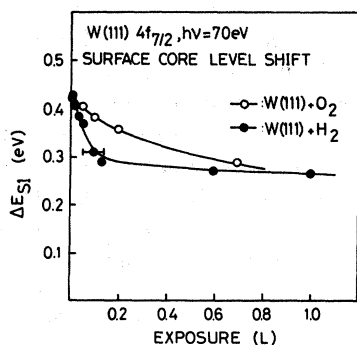


FIG. 3. Surface-to-bulk core-level binding-energy difference ΔE_{S_1} for the topmost surface layer of W(111) as a function of exposure to hydrogen (solid circles) and oxygen (open circles).

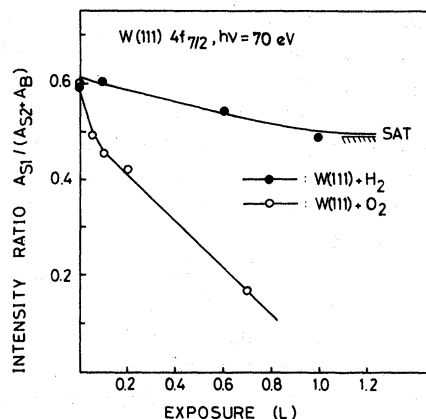


FIG. 4. Surface-to-bulk core-level intensity ratios (peak areas) for the topmost surface layer of W(111) as a function of exposure to hydrogen (solid circles) and oxygen (open circles).

of H_2 (uncorrected ion-gauge reading) corresponds to $\sim 7 \times 10^{14}$ atoms/cm² striking the surface (taking an ion-gauge sensitivity for H_2 of 0.4). If it is assumed that the sticking probability is ~ 0.8 ,¹⁸ this exposure corresponds to a coverage of $\sim 5.6 \times 10^{14}$ atoms/cm², which is nearly equal to the number of atoms in the first surface plane (5.8×10^{14} atoms/cm²). The change in S_1 binding energy appears to correlate with the quenching and lowering in binding energy of valence-band surface states recently observed for W(111) by Cerrina *et al.*¹⁹ in the same range of H_2 exposures. Surface states from other transition metals such as Ni(111) are also known to be strongly affected by hydrogen adsorption and to change their binding energy continuously, even long before full coverage is reached.²⁰ Such changes in the valence-band density-of-states distribution, which accompany a charge transfer from substrate to hydrogen atoms, lower the initial-state electrostatic potential felt by the 4f core electron. The fact that the chemical shift is *continuous* further supports our interpretation in terms of valence-band surface-state quenching and binding-energy changes. By contrast, a purely *local* chemisorption bond model is not consistent with our data, since it should predict two core levels at different binding energy, one level originating from uncovered surface atoms and another chemically shifted level from atoms bonded to hydrogen.

For saturation coverage, S_1 has lost 11% of its intensity to the main peak, which thereby has shifted to 25 meV higher binding energy. This suggests a chemical shift of ~ 0.4 eV for a small

portion of the first layer. We also note that both surface and bulk core levels are slightly broadened by 20–30 meV with respect to the clean surface. These more subtle changes may be attributed to the occupation of inequivalent binding sites, as is also suggested by the occurrence of multiple peaks in thermal desorption spectra.²¹

Finally, we note that the chemical shift for the hydrogen-saturated W(111) surface is 75 meV larger than for W(100).¹⁰ This suggests that *three* hydrogen atoms are bridge-bonded to one top-layer atom (Fig. 2), compared to only *two* hydrogen atoms for the W(100) surface. This number is also consistent with thermal desorption measurements of the saturation coverage at 300 K.²² Submonolayer coverage of hydrogen on W(100) induces surface core-level shifts that are partly due to surface reconstruction and partly chemical in origin. A detailed core-level spectroscopy study of the hydrogen-induced W(100) surface reconstruction has been published elsewhere.¹⁰

B. W(111)+O₂, W(100)+O₂

The effect of oxygen chemisorption on W(111) at 300 K is different from that of hydrogen, in that surface core-level S_1 is quenched, instead of merely shifted (Fig. 5). While being quenched, S_1 moves continuously to higher binding energy by about the same amount as has also been found for hydrogen chemisorption (open circles in Fig. 3). Similar to the case for hydrogen, the continuous shift probably also arises from initial-state changes in the surface density of states, affecting also uncovered surface atoms. The quenching is accompanied by the growth of a broad shoulder (*A*) at 0.4–0.5 eV higher binding energy than the bulk peak. This indicates the formation of a more local chemisorption bond, by which valence charge is directly transferred from the W substrate atoms to the oxygen atoms. After saturating the surface with oxygen (~ 2 -L exposure), peak *A* has become more pronounced, and S_1 has disappeared (Fig. 6, Table I). LEED and electron-stimulated desorption^{23–25} as well as angle-resolved photoemission from the valence band²⁶ suggest that oxygen adsorbs disorderedly on W(111) at room temperature. This is consistent with the large width of the surface core level *A* in Figs. 5 and 6. We do not find any evidence for a change in the oxygen site from bridge to on top with increasing coverage as suggested in Ref. 25.

Oxygen chemisorption on W(100) has been stud-

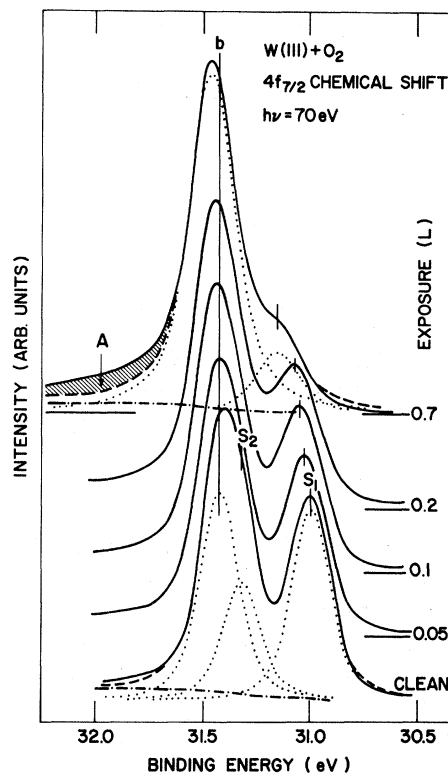


FIG. 5. Angle-integrated $4f_{7/2}$ core-level emission spectra for W(111) as a function of oxygen coverage (solid lines). A linear background has been subtracted. Dotted lines show best-fit decompositions into Lorentzian bulk (*b*) and surface core levels (S_1, S_2), convoluted with the instrument resolution. A small extrinsic background is also shown (dash-dotted lines). The result of our line-shape fit is shown by a dashed curve, only where it deviates from the experimental curve.

ied by LEED,²⁷ electron-stimulated desorption (ESD),²⁸ and low-energy electron-loss spectroscopy (LEELS).²⁹ For 0.5-ML (ML denotes monolayer) coverage a two-domain $P(4 \times 1)$ LEED pattern has been observed which has been related to the formation of double rows of chemisorbed oxygen atoms.²⁷ Figure 7 shows the corresponding $4f_{7/2}$ core level (including secondary electron background), for which a coverage of 0.5 ML has been deduced from the measured work-function change $\Delta\Phi = 0.57$ eV (using the calibration of Ref. 27). Again, a broad feature is seen at the high-binding-energy side of the bulk peak, as for W(111), and the intrinsic surface core level has completely been quenched. Upon annealing to ~ 1100 K, the work function reduces to a value 170 meV below that for the clean surface, in agreement with Ref. 27, and a much better defined surface core peak (*C*) shows

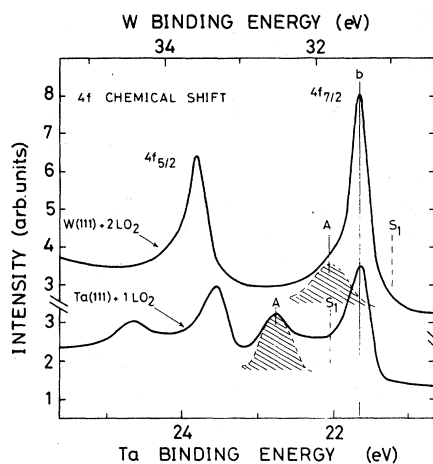


FIG. 6. Angle-integrated 4f core-level emission spectra for W(111) and Ta(111) after monolayer chemisorption of oxygen. Exposure of W(111) to 2 L of oxygen gives approximately saturation coverage. The curve for Ta(111) (1-L O₂ exposure) has been taken just before the onset of in-depth surface oxidation (see also Fig. 10). The dashed lines mark the positions of the clean surface core levels, peaks A are chemically shifted surface levels.

up at 0.53 eV higher binding energy than the bulk peak (Fig. 7). This corresponds with a chemical shift of $0.53 + 0.35 = 0.88$ eV with respect to the intrinsic surface core-level position at 0.35 eV lower binding energy. The negative work-function change and the accompanying change of the LEED pattern into a $p(2 \times 1)$ structure has been ascribed to a place exchange of oxygen atoms with every second W atom, leading to the formation of single rows of oxygen atoms.^{27,29} Thus, the core peak C arises from W atoms surrounded by oxygen atoms, which are incorporated in the first layer. We note that these chemical shifts cannot be the

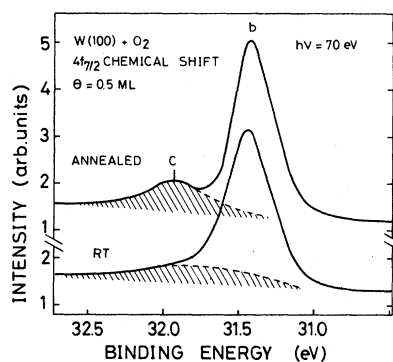


FIG. 7. Angle-integrated photoemission curves of 4f core levels for 0.5 monolayer of oxygen on W(100), before and after annealing to ~ 1100 K.

result of in-depth surface oxidation, since they are much less than the 4f binding-energy shift of 4.3 eV, measured for bulk WO₃.⁴

C. Ta(111)+H₂

Photoemission curves of Ta 4f_{7/2} and 4f_{5/2} core levels are shown in Fig. 8 (including secondary-electron background). The intrinsic surface core levels are found at the opposite side of the bulk core peak, thus 4f electrons from surface atoms of Ta are more tightly bound than from bulk atoms. This interesting sign reversal in the surface shift between Ta and W, which are neighboring elements in the 5d row, has been experimentally demonstrated and explained in Ref. 9. Again, the 4f_{5/2} levels at 1.90 eV higher binding energy will not be further considered since they are a replica of the 4f_{7/2} levels apart from a ~ 36 -meV extra lifetime broadening.

Similar to W(111), there are two intrinsic surface core levels S₁ and S₂ from the first and second (third) layers of Ta(111), which move continuously

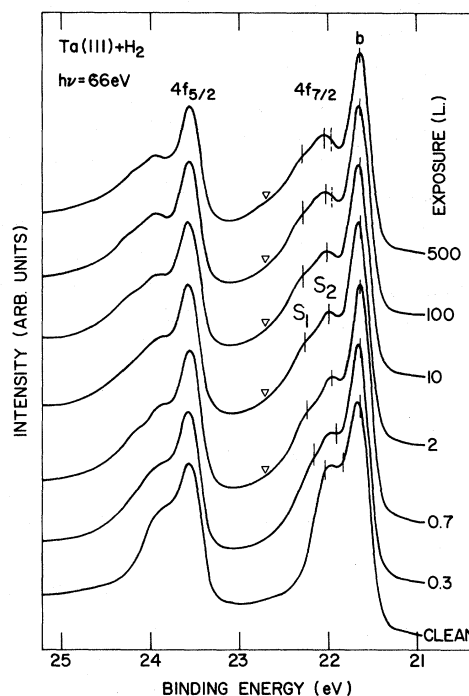


FIG. 8. Angle-integrated 4f core-level emission spectra for Ta(111) covered with hydrogen, showing core-level positions for bulk (b) and surface (S₁, S₂) atoms. Triangles mark a weak shoulder due to a small oxygen contamination.

to higher binding energies for increasing hydrogen exposure (Fig. 9). The second layer shift can be seen as a separate peak, because it is further removed from the bulk peak. Surface chemical shifts for saturation coverage of hydrogen are 210 and 170 meV for S_1 and S_2 , respectively, slightly larger than for W(111) (Table I). Again, most of this chemical shift occurs during the first stage of chemisorption (<0.3 L). Thus the same conclusions that have been drawn for W(111)+H₂ also apply for Ta(111). The triangles in Fig. 8 mark a weak shoulder at a binding energy of 22.7 eV, which we ascribe to a small contamination of oxygen (Sec. III D).

D. Ta(111)+O₂

The spectral changes during the initial stages of oxygen chemisorption on Ta(111) at 300 K are similar to those observed for W(111) (Fig. 10). Chemical shifts and intensity changes can be followed more easily for Ta(111) because the surface core peaks are further removed from the bulk peak by chemisorption. S_1 and S_2 are both quenched, while a new peak A grows in intensity. At 1-L exposure A has reached full intensity and the intrinsic core levels have been completely quenched. Its chemical shift with respect to S_1 is 0.72 eV, close to the 0.88-eV shift for W(111). Figure 6 shows these spectra for comparison. Thus, peak A likely represents the same binding state for both elements. After 5-L exposure at 300 K, new structures C , D , and E have replaced A , while the bulk core level is attenuated and the secondary electron background is increased. These dramatic changes strongly suggest that oxygen penetrates the first

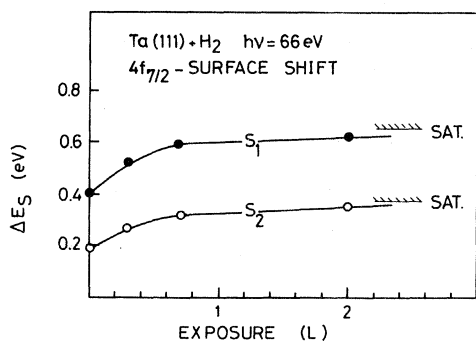


FIG. 9. Surface-to-bulk core-level binding energy differences for top layer atoms (S_1) and second (third) layer atoms (S_2) in Ta(111) as a function of hydrogen coverage.

layers of the crystal, marking the onset of surface oxidation. Peaks D , C , and E are shifted by 2.4, 1.3, and 0.5 eV relative to the bulk peak. The presence of three smeared structures on top of a high background points at the presence of different suboxides and a high degree of surface disorder. This is also consistent with the complete absence of any LEED spots. Presently, no further conclusion can be drawn about the state of oxidation of the surface, since to our knowledge, no experimental data are available on $4f$ binding-energy shifts for the different bulk oxides. By contrast, the W(111) surface did *not* oxidize at 300 K in the exposure range studied (maximum exposure of 11 L).

IV. DISCUSSION

The continuous substrate core-level shifts observed for hydrogen adsorption cannot be explained

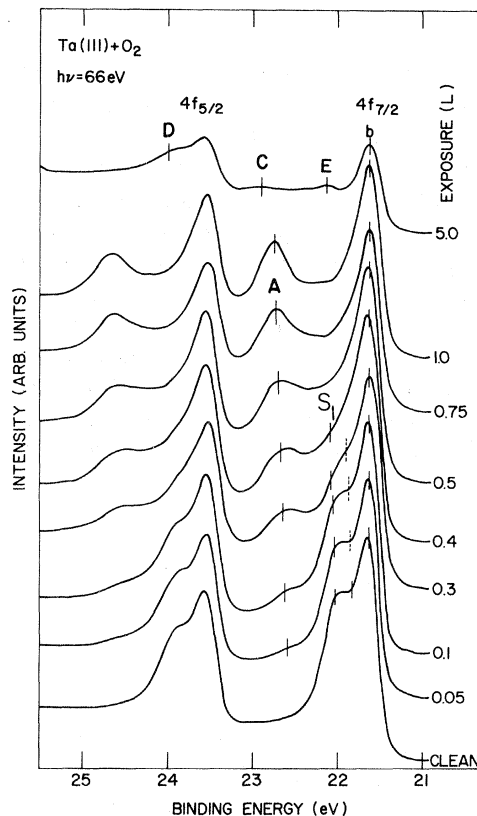


FIG. 10. Angle-integrated $4f$ core-level emission spectra for Ta(111) as a function of oxygen coverage, showing the quenching of S_1 and S_2 and the growth of new chemically shifted substrate peaks A , C , D , and E . Note that D is a chemically shifted $4f_{7/2}$ level.

by a simple XPS—chemical-bonding model in which the core-level binding energy directly reflects the local chemical environment. Instead, such continuous shifts appear to correlate with the quenching of surface states in the valence band. On the other hand, oxygen chemisorption yields continuous shifts as well as discrete new peaks, which reflect a more localized and drastic change in the electrostatic potential at the atomic core. Hydrogen adsorption on stepped surfaces represents a special case of such localization. Step and terrace atoms on Ir(332) have been shown to have different 4f binding energies.³⁰ Preferential adsorption of hydrogen at the step edges shifted the step-atom core level by ~ 0.25 eV to higher binding energy, but left the terrace-atom core peak unaffected. This chemical shift appears to correlate with the quenching of the step-related surface states in the valence band.³⁰

The question arises; to what extent possible differences in final-state screening of the core hole also affect substrate core-level binding energies. Final-state relaxation effects have always been a complicating factor in XPS analyses of solids, and relaxation shifts between free atoms and bulk atoms are typically several eV.³¹

However, differences in relaxation shifts between *surface* and *bulk* atoms are probably small for 5d metals, since full core-hole screening is expected to be operative for both bulk³² and surface atoms due to the short Debye screening lengths. Indeed, initial-state changes alone can largely account for the observed trends in the intrinsic 5d metal surface shifts, such as the crystallographic dependencies and the sign reversal between Ta and W.^{9,33} The substrate relaxation shifts for fractional monolayer coverages are expected to be about the same as for the clean surfaces for the same reason. Final-state effects may, however, be significant for monolayer adsorption (peak A in Figs. 5, 6, and 10; C in Fig. 7), and, of course, surface oxidation (C, D, and E in Fig. 10) where the density of conduction electrons (and thereby the Debye screening length) is reduced substantially.

Of particular interest is the question why all chemical shifts observed to date are toward larger binding energy (i.e., away from E_F). Surface shifts of this sign have now been seen for hydrogen or oxygen chemisorption on the low-index surfaces of W, on Ta(111), and the surfaces of Ir,¹⁴ and for CO on Pt.³⁴ In a purely initial-state model, it immediately follows that electronic charge is transferred from the substrate atom to the more

electronegative hydrogen or oxygen atom. The fact that the Ta and W bulk core levels remain unshifted to within 40 meV throughout the entire exposure range without significant loss of intensity implies that the charge transfer is spatially confined to the substrate layers to which the adsorbate atoms are bonded. This eliminates charge transfer from the *bulk* as a cause for the absence of a measurable shift in earlier XPS work.³⁵

The sign of the chemisorption shift may also be understood by use of a semi-empirical thermodynamical model,³⁶ which includes final-state relaxation effects. This model explains the sign reversal in the intrinsic surface shift between Ta and W (Ref. 37) and points at an interesting correspondence between surface core-level shifts and heats of segregation.³⁸ The core-ionized site is assumed to be fully screened by the surrounding electrons. Thus, the final state can be treated as a $(Z + 1)$ impurity dissolved in the Z host metal. It can then be shown that the intrinsic surface-to-bulk core-level binding energy difference is approximately given by the difference in surface energies:

$$\Delta E(Z) = E_S(Z + 1) - E_S(Z), \quad (1)$$

where the surface energy $E_S(Z)$ for element Z is the difference between bulk and surface cohesive energy. The heat of solution of the $(Z + 1)$ impurity in the Z metal has been neglected in Eq. (1) because it is generally small between neighboring elements.³⁹ Since the surface energy is known to vary parabolically through a transition series, Eq. (1) correctly predicts a change in sign between Ta and W. Namely, for early transition metals such as Ta the surface shift is positive, because the gain in bonding in the final state (W) is larger for a bulk atom than for a surface atom, whereas for nearly-filled metals the situation is the reverse. Thus the measured surface-to-bulk core-level binding-energy differences are roughly equal to the heats of segregation for element $(Z + 1)$ diluted in Z metal. Consequently, in a W_xTa_{1-x} alloy Ta would segregate to the surface, while for Re_xW_{1-x} and Pt_xIr_{1-x} alloys Re and Pt would segregate. Pt does indeed segregate to the surface of an Pt_xIr_{1-x} alloy, according to a recent Auger spectroscopy study, in which the surface concentration has directly been measured.⁴⁰ In the presence of an adsorbate, Eq. (1) should be modified as⁴¹

$$\Delta E(Z) = E_S(Z + 1) - E_S(Z) - \Delta H_{\text{chem}}, \quad (2)$$

where $\Delta H_{\text{chem}} = H(Z + 1) - H(Z)$ is the difference

between chemisorption energies for the adsorbate on elements ($Z + 1$) and Z . This follows from a highly simplified bond-breaking model, in which all broken bonds at the surface are replaced by bonds to adsorbate atoms. Given the rather crude approximations involved, Eq. (2) may only be used as a qualitative guide. As a general trend, chemisorption energies decrease as one goes from left to right in a transition metal series.⁴² Consequently, Eq. (2) predicts a chemical shift toward higher binding energies, in agreement with our experimental observations.

There is again an interesting correspondence between surface chemical shifts and chemisorption-induced surface segregation. Consider, for example, adsorption of hydrogen on Ir. The chemisorption energy of hydrogen on Pt surfaces is somewhat lower than on Ir [by ~ 0.26 eV/atom for the (111) surface].⁴³ Then Eq. (2) predicts a chemical shift toward higher binding energy but no change of sign, in agreement with the core-level measurements of Ref. 14. In other words, the gain in bonding in the final state (Pt) becomes less for hydrogen-covered surface atoms, thus less Pt would segregate to the surface of a dilute $\text{Pt}_x\text{Ir}_{1-x}$ alloy ($x \ll 1$) if a monolayer of hydrogen is present. Similarly, chemisorption of hydrogen or oxygen induces extra enrichment of Ta at the surface of $\text{W}_x\text{Ta}_{1-x}$ alloy [$H(\text{W}) < H(\text{Ta})$] (Refs. 42 and 44) in Eq. (2) (Ref. 36)] but less segregation of Re for hydrogen-covered $\text{Re}_x\text{W}_{1-x}$. A reversal in segregation is expected for oxygen-covered $\text{Re}_x\text{W}_{1-x}$, since the W surface shift changes sign upon monolayer adsorption of oxygen. Other techniques by which surface concentrations are directly measured give little information on chemisorption-induced surface segregation for the alloys discussed above. Recently, heats of surface segregation have been calculated for various overlayer-alloy combinations,⁴¹ using experimental chemisorption bond

energies and semiempirical surface energies.⁴⁵ This calculation supports our predictions for dilute $\text{Pt}_x\text{Ir}_{1-x}$ alloys.

In conclusion, substrate core-level spectroscopy is a promising technique for chemisorption studies, and can be used as a monitor of surface oxidation and surface coverage. In addition, chemical shifts are sensitively dependent on the binding site of the adsorbate atom, as has been shown for O/W(001) in Fig. 7. Theoretically, initial-state chemical core shifts have been obtained for a monolayer of hydrogen on Sc and Ti(0001) surfaces, by use of a self-consistent scheme for calculation of the surface electronic structure.⁴⁶ Interestingly, these authors found a "healing" of the Sc and Ti core spectra; i.e., intrinsic surface core levels are deeper than the bulk ones, as for Ta, but a H monolayer with H at threefold sites reduces the surface core-level shifts again to zero. This behavior is opposite to what we have seen for hydrogen adsorption on Ta. The reason for this difference is not yet clear. Unfortunately, no calculations are yet available for $5d$ metal chemical shifts. Such self-consistent schemes may be used in comparison with experimental data to determine binding sites of adsorbate atoms. Of course, a quantitative comparison will only be meaningful if the possible role of final-state relaxation shifts is better understood.

ACKNOWLEDGMENTS

We wish to thank A. Marx, J.J. Donelon, and the staff of the University of Wisconsin's Synchrotron Radiation Center for their capable help. One of us (J.F. van der Veen) acknowledges stimulating discussions with Dr. A.R. Miedema. This work was supported in part by the U.S. Air Force Office of Scientific Research (AFOSR) under Contract No. F-49620-81-C-0089.

¹K. Siegbahn, University of Uppsala Institute of Physics Publication No. 940 (Uppsala, Sweden, 1976) (unpublished).
²J. C. Fuggle and D. Menzel, *Surf. Sci.* **53**, 21 (1975).
³A. Barrie and A. M. Bradshaw, *Phys. Lett.* **55A**, 306 (1975).
⁴T. A. Carlson and G. E. McGuire, *J. Electron. Spectrosc. Relat. Phenom.* **1**, 161 (1972).
⁵C. R. Brundle, *J. Vac. Sci. Technol.* **11**, 212 (1974).
⁶S. A. Flodström, C. W. B. Martinsson, R. Z. Bachrach, S. B. M. Hagström, and R. S. Bauer, *Phys. Rev. Lett.*

40, 907 (1978).

⁷C. M. Garner, I. Lindau, C. Y. Su, P. Pianetta, and W. E. Spicer, *Phys. Rev. B* **19**, 3944 (1979).

⁸P. Pianetta, I. Lindau, C. M. Garner, and W. E. Spicer, *Phys. Rev. B* **18**, 2792 (1978).

⁹J. F. van der Veen, P. Heimann, F. J. Himpsel, and D. E. Eastman, *Solid State Commun.* **37**, 555 (1981).

¹⁰J. F. van der Veen, F. J. Himpsel, and D. E. Eastman, *Solid State Commun.* **40**, 57 (1981).

¹¹G. Treglia, M. C. Desjonquères, D. Spanjaard, Y. Laspailly, C. Guillot, Y. Jugnet, Tran Minh, Duc, and J.

- Lecante, *J. Phys. C* **14**, 3463 (1981).
- ¹²P. H. Citrin, G. K. Wertheim, and Y. Baer, *Phys. Rev. Lett.* **41**, 1425 (1978).
- ¹³T. M. Duc, C. Guillot, Y. Lassailly, J. Lecante, Y. Jugnet, and J. C. Vedrine, *Phys. Rev. Lett.* **43**, 789 (1979).
- ¹⁴J. F. van der Veen, F. J. Himpsel, and D. E. Eastman, *Phys. Rev. Lett.* **44**, 189 (1980).
- ¹⁵D. E. Eastman, J. J. Donelon, N. C. Hien, and F. J. Himpsel, *Nucl. Instrum. Methods* **172**, 327 (1980).
- ¹⁶M. K. Debe and D. A. King, *Surf. Sci.* **81**, 193 (1979).
- ¹⁷T. E. Felter, R. A. Barker, and P. J. Estrup, *Phys. Rev. Lett.* **38**, 1138 (1977).
- ¹⁸P. W. Tamm and L. D. Schmidt, *J. Chem. Phys.* **55**, 4253 (1971); these authors measured ratios of initial sticking coefficients on various low index surfaces and found $S_0(111)/S_0(100)=1.3$. Using an $S_0(100)$ value of 0.6 (Ref. 22), we obtain $S_0(111)\simeq 0.8$.
- ¹⁹F. Cerrina, J. Anderson, G. J. Lapeyre, O. Bisi, and C. Calandra, *Phys. Rev. B* **25**, 4949 (1982).
- ²⁰F. J. Himpsel, J. A. Knapp, and D. E. Eastman, *Phys. Rev. B* **19**, 2872 (1979).
- ²¹T. E. Madey, *Surf. Sci.* **29**, 571 (1972).
- ²²Tamm and Schmidt (Ref. 18) measured by flash desorption a saturation coverage of 1.3×10^{15} atoms/cm² at 300 K (only the β_3 and β_4 states are filled). In this study absolute coverages have been obtained by using a coverage of 1.5×10^{15} atoms/cm² for a hydrogen monolayer on $W(100)$ as a reference. A recent experiment by D. A. King and G. Thomas [*Surf. Sci.* **92**, 201 (1980)] has yielded 1.9×10^{15} atoms/cm² for the (100) surface. Using the latter number, one obtains for the (111) surface a saturation coverage of $\sim 1.6 \times 10^{15}$ atoms/cm², which corresponds to ~ 2.8 hydrogen atoms per W surface atom.
- ²³N. J. Taylor, *Surf. Sci.* **2**, 544 (1964).
- ²⁴T. E. Madey, J. J. Czyzewski, and J. T. Yates, Jr., *Surf. Sci.* **57**, 580 (1976).
- ²⁵H. Niehus, *Surf. Sci.* **80**, 245 (1979).
- ²⁶R. Avci, G. J. Lapeyre, R. Rosei, and J. Anderson, in *Conference Digest of the VI International Conference on Vacuum Ultraviolet Radiation Physics, Charlottesville, 1979* (in press), Contribution I-13; R. Avà and G. J. Lapeyre, *Phys. Rev. Lett.* (unpublished).
- ²⁷H. M. Kramer and E. Bauer, *Surf. Sci.* **92**, 53 (1980); **93**, 407 (1980), and references cited therein.
- ²⁸T. E. Madey, J. J. Czyzewski, and J. T. Yates, *Surf. Sci.* **49**, 46 (1975).
- ²⁹H. Froitzheim, H. Ibach, and S. Lehwald, *Phys. Rev. B* **14**, 1362 (1976).
- ³⁰J. F. van der Veen, D. E. Eastman, A. M. Bradshaw, and S. Holloway, *Solid State Commun.* **39**, 1301 (1981).
- ³¹A. R. Williams and N. D. Lang, *Phys. Rev. Lett.* **40**, 954 (1978).
- ³²J. C. Fuggle, M. Campagna, Z. Zolnieriek, R. Lässer, and A. Platau, *Phys. Rev. Lett.* **45**, 1597 (1980).
- ³³M. C. Desjonquères, D. Spanjaard, Y. Lassailly, C. Guillot, *Solid State Commun.* **34**, 807 (1980).
- ³⁴R. C. Baezhold, G. Apai, E. Shusotrovich, and R. Jaeger, SSRL Activity Report, Stanford, 1981, p. 120 (unpublished); M. L. Shek, P. M. Stefan, I. Lindau, and W. E. Spicer, *J. Vac. Sci. Technol.* **20**, 879 (1982).
- ³⁵C. R. Brundle, *Surf. Sci.* **48**, 99 (1975).
- ³⁶B. Johansson and N. Mårtensson, *Phys. Rev. B* **21**, 4427 (1980).
- ³⁷A. Rosengren and B. Johansson, *Phys. Rev. B* **22**, 3706 (1980).
- ³⁸A. Rosengren and B. Johansson, *Phys. Rev. B* **23**, 3852 (1981).
- ³⁹A. R. Miedema, *J. Less-Common Met.* **41**, 283 (1975).
- ⁴⁰F. J. Kuijers and V. Ponec, *Appl. Surf. Sci.* **2**, 43 (1978).
- ⁴¹D. Tománek, S. Mukherjee, V. Kumar, and K. H. Bennemann, *Solid State Commun.* **41**, 273 (1982).
- ⁴²I. Toyoshima and G. A. Somorjai, *Catal. Rev. Sci. Eng.* **19**, 105 (1979).
- ⁴³G. Ertl, in *The Nature of the Surface Chemical Bond*, edited by T. N. Rhodin and G. Ertl (North-Holland, Amsterdam, 1979).
- ⁴⁴S. M. Ko and L. D. Schmidt, *Surf. Sci.* **42**, 508 (1974).
- ⁴⁵A. R. Miedema, *Z. Metallkd.* **69**, 455 (1978).
- ⁴⁶P. J. Feibelman and D. R. Hamann, *Solid State Commun.* **34**, 215 (1980).